Supplemental Material: Steady Rayleigh–Bénard convection between stress-free boundaries

Baole Wen, David Goluskin, Matthew LeDuc, Gregory P. Chini, and Charles R. Doering

Table S1 gives numerical values of the asymptotic prefactors in expression (3.1) for the steady rolls constructed in the asymptotic analysis of Chini & Cox (2009). Tables S2 and S3 give the Nu and $RePr$ values plotted in figure 2. Table S4 compares steady rolls to unsteady rolls with the same mean aspect ratio from the DNS of Wang *et al.* (2020).

Figure S1 shows the normalized dissipation profiles $\overline{\varepsilon}(z)/\langle\varepsilon\rangle$ of steady rolls at various Pr for Ra values of 5×10^6 and 10^9. There is much less variation with Pr at the larger Ra value, reflecting the Pr-independence that is predicted in the $Ra\to\infty$ asymptotic limit. Only the $Pr = 100$ profile is significantly different from the others when $Ra = 10^9$; convergence to asymptotic behaviour as $Ra\to\infty$ is slower at larger Pr (cf. figure 1).

$k = 2\pi/\Gamma$	$c_n(k)$	$c_r(k)$	$k = 2\pi/\Gamma$	$c_n(k)$	$c_r(k)$
0.25	0.09084366	0.08479653	5.25	0.26516638	0.07042333
0.5	0.13783563	0.10165665	5.5	0.26383550	0.06791123
0.75	0.17242486	0.11048428	5.75	0.26253039	0.06554476
1	0.19909232	0.11516486	6	0.26126222	0.06331554
1.25	0.21981992	0.11716681	6.25	0.26003730	0.06121496
1.5	0.23579393	0.11727251	6.5	0.25886080	0.05923472
1.75	0.24788488	0.11600002	6.75	0.25773340	0.05736652
2	0.25681088	0.11373790	7	0.25665667	0.05560274
2.25	0.26318917	0.11079160	7.25	0.25563005	0.05393607
2.5	0.26754979	0.10740171	7.5	0.25465196	0.05235964
2.75	0.27033921	0.10375413	7.75	0.25372157	0.05086718
3	0.27192661	0.09998906	8	0.25283657	0.04945277
3.25	0.27260954	0.09620876	8.25	0.25199552	0.04811103
3.5	0.27262477	0.09248559	8.5	0.25119483	0.04683679
3.75	0.27215669	0.08886847	8.75	0.25043350	0.04562556
4	0.27134834	0.08538889	9	0.24970964	0.04447307
4.25	0.27030747	0.08206516	9.25	0.24902004	0.04337532
4.5	0.26911578	0.07890636	9.5	0.24836456	0.04232885
4.75	0.26783386	0.07591494	9.75	0.24773960	0.04133018
5	0.26650668	0.07308893	10	0.24714363	0.04037628

Table S1: Numerical values of the asymptotic prefactors c_n and c_r in (3.1) for various wavenumbers k. Values of c_n are from the data of Chini & Cox (2009), and c_r is calculated from c_n according to (A 5).

Ra	$N_x \times N_z$	Nu $Pr = 10^{-2}$	$Pr = 10^{-1}$	$Pr = 1$	$Pr = 10$	$Pr = 10^2$
10^3	128×65	1.46630	1.46614	1.46687	1.46716	1.46718
$10^{13/4}$	128×65	2.37255	2.37025	2.36637	2.37324	2.37425
$10^{14/4}$	128×65	3.18564	3.18049	3.15193	3.16265	3.16748
$10^{15/4}$	128×65	4.05203	4.04468	3.98471	3.96052	3.97220
10^4	128×65	5.07914	5.07051	4.98831	4.86435	4.88129
$10^{17/4}$	128×65	6.32515	6.31587	6.22172	5.94155	5.94945
$10^{18/4}$	128×65	7.83124	7.82158	7.72035	7.25591	7.21592
$10^{19/4}$	128×65	9.65227	9.64234	9.53590	8.89159	8.72489
10^5	128×65	11.8568	11.8467	11.7360	10.9457	10.5267
$10^{21/4}$	256×97	14.5268	14.5164	14.4021	13.5059	12.6816
$10^{22/4}$	256×97	17.7612	17.7506	17.6329	16.6557	15.2701
$10^{23/4}$	256×97	21.6798	21.6690	21.5483	20.5044	18.4060
10^6	256×97	26.4274	26.4164	26.2929	25.1935	22.2598
$10^{25/4}$	256×97	32.1797	32.1685	32.0425	30.8962	27.0879
$10^{26/4}$	256×97	39.1494	39.1379	39.0094	37.8234	33.2279
$10^{27/4}$	512×129	47.5938	47.5822	47.4514	46.2312	41.0104
10^7	512×129	57.8250	57.8132	57.6802	56.4307	50.7115
$10^{29/4}$	512×129	70.2211	70.2091	70.0740	68.7989	62.6608
$10^{30/4}$	512×129	85.2397	85.2277	85.0905	83.7928	77.2962
$10^{31/4}$	512×129	103.437	103.424	103.285	101.967	95.1593
10^8	512×129	125.484	125.472	125.330	123.991	116.909
$10^{33/4}$	768×193	152.192	152.179	152.036	150.683	143.355
$10^{34/4}$	1024×193	184.554	184.541	184.394	183.026	175.477
$10^{35/4}$	1024×257	223.758	223.745	223.599	222.215	214.465
10^9	1024×257	271.266	271.253	271.105	269.698	261.773
$10^{37/4}$	1280×257		328.798	328.713	327.238	319.134
$10^{38/4}$	1280×257		398.523	398.427	397.003	388.734
$10^{39/4}$	1536×257		483.062	482.910	481.470	473.049
10^{10}	1792×257		585.437	585.285	583.841	575.311
$10^{41/4}$	2048×321				707.958	699.254
$10^{42/4}$	2560×321				858.111	849.325
$10^{43/4}$	3072×321				1040.21	1031.35
10^{11}	3584×321					1251.98

Table S2: Values of the Nusselt number (Nu) plotted in figure 2(a) for steady rolls of aspect ratio $\Gamma = 2$ ($k = \pi$). The resolution of Fourier modes (N_x) and Chebyshev collocation points (N_z) is given also.

Ra	$N_x \times N_z$			$RePr$		
		$Pr = 10^{-2}$	$Pr = 10^{-1}$	$Pr = 1$	$Pr = 10$	$Pr = 10^2$
10^3	128×65	4.860211	4.859365	4.863013	4.864534	4.864669
$10^{13/4}$	128×65	11.11289	11.10342	11.08274	11.10817	11.11225
$10^{14/4}$	128×65	18.64998	18.62765	18.48547	18.50202	18.52133
$10^{15/4}$	128×65	29.18438	29.14861	28.81749	28.56985	28.61439
10^4	128×65	44.44510	44.39718	43.87005	42.81088	42.85149
$10^{17/4}$	128×65	66.65392	66.59490	65.87916	63.22068	63.10225
$10^{18/4}$	128×65	99.00479	98.93476	98.02324	92.79036	92.04534
$10^{19/4}$	128×65	146.2211	146.1395	145.0123	136.1512	133.5699
10^5	128×65	215.2057	215.1114	213.7389	200.3372	193.1899
$10^{21/4}$	256×97	316.0649	315.9563	314.2983	295.6302	278.8445
$10^{22/4}$	256×97	463.6093	463.4841	461.4878	436.6766	402.1873
$10^{23/4}$	256×97	679.5490	679.4041	677.0022	644.8536	580.6680
10^6	256×97	995.7158	995.5474	992.6546	951.6627	841.1621
$10^{25/4}$	256×97	1458.790	1458.594	1455.104	1403.377	1226.322
$10^{26/4}$	256×97	2137.241	2137.009	2132.789	2067.960	1803.793
$10^{27/4}$	512×129	3131.499	3131.224	3126.109	3045.229	2674.566
10^7	512×129	4588.895	4588.574	4582.361	4481.765	3981.512
$10^{29/4}$	512×129	6725.606	6725.221	6717.660	6592.805	5932.137
$10^{30/4}$	512×129	9858.786	9858.334	9849.112	9694.374	8833.901
$10^{31/4}$	512×129	14453.85	14453.31	14442.05	14250.46	13140.24
10^8	512×129	21193.84	21193.21	21179.44	20942.25	19519.46
$10^{33/4}$	768×193	31080.45	31079.68	31062.85	30769.81	28954.88
$10^{34/4}$	1024×193	45585.16	45584.26	45563.33	45201.19	42895.45
$10^{35/4}$	1024×257	66865.43	66864.32	66839.10	66391.72	63471.97
10^9	1024×257	98091.13	98089.85	98058.98	97504.78	93819.57
$10^{37/4}$	1280×257		143906.3	143882.5	143186.5	138542.0
$10^{38/4}$	1280×257		211139.3	211107.6	210266.2	204428.0
$10^{39/4}$	1536×257		309825.2	309769.0	308731.1	301407.4
10^{10}	1792×257		454641.9	454573.4	453293.9	444122.9
$10^{41/4}$	2048×321				665545.3	654078.8
$10^{42/4}$	2560×321				977028.2	962715.7
$10^{43/4}$	3072×321				1434327	1416484
10^{11}	3584×321					2083475

Table S3: Values of the Péclet number ($RePr$) plotted in figure 2(b) for steady rolls of aspect ratio $\Gamma = 2$ ($k = \pi$). The resolution of Fourier modes (N_x) and Chebyshev collocation points (N_z) is given also.

Ra	Steady roll Nu	Steady roll Re	DNS Nu	DNS Re
10^7	53.2089	515.276	48.53	488.77
3×10^7	77.5286	1080.31	69.43	1016.46
10^8	116.711	2425.10	96.81	2202.08
3×10^8	169.146	5063.63	134.00	4552.41
10^9	253.606	11332.6	198.01	10135.1

Table S4: Comparison of Nu and Re between steady rolls with fixed aspect ratio $\Gamma = 3.2$ and unsteady DNS by Wang *et al.* (2020) with the same mean aspect ratio. In both cases $Pr = 10$.

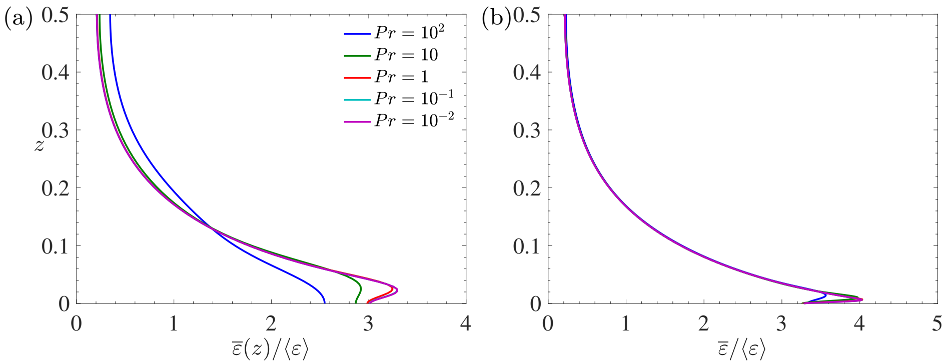

Figure S1: Horizontally averaged dissipation profiles normalized by their volume averages, $\overline{\varepsilon}(z)/\langle\varepsilon\rangle$, for steady convective rolls at (a) $Ra = 5 \times 10^6$ and (b) $Ra = 10^9$ with $\Gamma = 2$ and various Pr. Only half of the vertical domain is shown ($0 \leqslant z \leqslant 0.5$) because the profiles are symmetric about the mid-plane.

REFERENCES

Chini, G.P. & Cox, S.M. 2009 Large Rayleigh number thermal convection: Heat flux predictions and strongly nonlinear solutions. *Physics of Fluids* **21**, 083603.

Wang, Q., Chong, K.-L., Stevens, R.J.A.M., Verzicco, R. & Lohse, D. 2020 From zonal flow to convection rolls in Rayleigh–Bénard convection with free-slip plates. *arXiv:2005.02084* .